CrystEngComm

Accepted Manuscript

ROYAL SOCIETY OF CHEMISTRY

www.rsc.org/crystengcomm

CrystEngComm

ARTICLE

Synthesis of calcium phosphate crystals with thin nacreous structure

Received 00th January 20xx,
Accepted 00th January 20xx

DOI: 10.1039/x0xx00000x

www.rsc.org/

Song Chen,[a] Kathryn Grandfield,[b] Shun Yu,[c] Håkan Engqvist[a] and Wei Xia*[a]

Nacre-like structures have attracted great interest in recent years due to their outstanding toughness, stiffness and impact resistance. However, there is a challenge associated with engineering nacre-like calcium phosphate crystals. In this study, thin nacreous-like monetite sheets were synthesized in solutions guided by surfactant. The influence of temperature, initial pH, Ca/P ratio, stirring time and the concentration of cetyl-trimethyl ammonium bromide (CTAB) on the nacre-like structure has been studied. Findings showed that a nacre-like structure could only be formed at high temperature (90 ℃), high initial pH (11), sufficient stirring time (3 h), and under the presence of CTAB. Small-angle X-ray scattering experiment carried out at synchrotron radiation facility showed the distance between nano layers was around 2.6 nm and TEM confirmed the fine sheet-like structure. The mechanism of forming the nacre-like structure and its characterization was discussed.

1. Introduction

Among many natural hierarchical nanostructures, nacre, due to its outstanding toughness, stiffness and impact resistance, has attracted much interest.[1] From the perspective of biomimetics, the well-organized layered structure is intriguing in terms of the self-assembly process guided by macro-molecules and nanostructures, and the mechanisms behind the synthetic and biomimetic processes. Different techniques [2-5] have been developed to synthesize nacre-like materials based on self-assembly processes. These bottom-up strategies have advantages in generating complex nanostructures on various scales compared to conventional top-down synthetic processes.[6, 7] One strategy is to use surfactants or macro-molecular as templates to guide the synthesis process. It is believed that the well-structured organization between inorganic and organic composites is required for the formation of these super structures. The molecules adsorbing on the surface of certain lattice planes can control crystal nucleation and growth. By using certain kinds of polymers/macro-molecular and controlling the concentration, materials with various shapes and nanostructures have been synthesized.[2] Using biomimetic approaches, nacre-like structures have been synthesized, such as calcium carbonate[8, 9], K_2SO_4-PAA[3], ZnO-polymer composites[4], and nacre retrosynthesis via amorphous precursor particles[5].

Calcium phosphate-based materials, because of their similarity to the composition, biodegradability, bioactivity, and osteoconductivity of bone mineral, have wide applications in teeth or bone replacement, bone repair and regeneration.[10] Monetite ($CaHPO_4$, DCPA) is one of the most stable calcium phosphate phases under acidic condition (pH below 4.8), while it is highly soluble in alkaline aqueous solution.[11] Monetite is a significant component of some calcium phosphate cements (CPC) and also used in some toothpastes, chewing gums and the food processing industry.[12, 13] It has demonstrated good osteoconductive properties in vitro and in vivo with applications in the orthopaedic and dental field.[14, 15] Furthermore, the rapid rate of bone formation on synthetic monetite makes it a promising bone regeneration material.[16, 17] Several distinct synthesis routes can be used for the preparation of monetite powder. The first method is to synthesis monetite by dehydrating brushite ($CaHPO_4{\cdot}2H_2O$) powder.[18] H. McDowell et al., prepared monetite by boiling 400 g $CaHPO_4{\cdot}2H_2O$ in 4 L of 0.07 M phosphoric acid for 72 hr.[19] J.G. Rabatin et al., found that anhydrous monetite can be formed by heating $CaHPO_4{\cdot}2H_2O$ at humid air or at three or more N_2 atmospheres at 135 ℃.[20] Solution-mediated method provides another route for the preparation of monetite, including a precipitation method[21], hydrothermal synthesis using monocalcium phosphate monohydrate (MCPM)[22] or calcium nitrate tetrahydrate, sodium dihydrogen phosphate and urea as precursors[23], and a sol-gel method[24, 25]. Other attempts to develop new synthesis methods include ball-milling in the solid state[26], spray-drying[27], membrane micro-dispersion mixing techniques using an oil-in-water system and a water-in-oil system[28], and reverse microemulsion[29, 30]. A variety of morphologies such as whiskers[22, 23], and flower-like petals[31] can be formed using different synthesis methods and parameters.

Although monetite with different morphologies and sizes has been prepared as mentioned above, there are no reports regarding the synthesis of monetite with a nacre-like structure. Recently, calcium phosphate-based materials with organized structures have been developed.[32] However, fabrication of

[a] Applied Materials Science, Department of Engineering Science, Uppsala University, Uppsala, Sweden
[b] Department of Materials Science and Engineering, McMaster University, Hamilton, Canada
[c] Polymeric materials & Wallenberg wood science center, Department of Fibre and Polymer Technology, KTH Royal Institute of Technology, Stockholm, Sweden

calcium phosphates with nacre-like structure is still a big challenge. In this paper, a simple commercial surfactant, CTAB, was used as a template to guide a self-assemble process of monetite crystals. Thin nacreous-like monetite crystals have been achieved by adjusting CTAB concentrations, the pH values of solutions, and temperature. A possible mechanism for this biomimetic self-assembly has been discussed.

2. Experimental

2.1 Sample preparation

For a typical experiment, solution 1 was prepared by dissolving 17.71 g $Ca(NO_3)_2{\cdot}4H_2O$, 1 g CTAB in 25 ml pure water. 1 ml $NH_3{\cdot}H_2O$ was added in the solution to adjust the pH value. Solution 2 was prepared by dissolving 7.49 g $(NH_4)_2HPO_4$ in anther beaker with 25 ml pure water. Solution 2 was dropped into solution 1 and the final solution was stirred at 90 °C for 3 h. The temperature, amount of CTAB, pH of precursor and Ca/P were varied to explore the influence of these parameters, see Table 1. The resultant powder was washed with ethanol and isolated by centrifugation. When preparing monetite in lower concentration precursor solutions, 0.59 g $Ca(NO_3)_2{\cdot}4H_2O$, 0.6 g CTAB and 1 g $NH_3{\cdot}H_2O$ were dissolved in 25ml pure water and 0.198 g $(NH_4)_2HPO_4$ was dissolved in another 25 ml pure water. $(NH_4)_2HPO_4$ solution was dropped into $Ca(NO_3)_2{\cdot}4H_2O$ solution and the final solution was stirred at 90 °C for 3 h.

Table 1 Variations of parameters during preparation

	T (°C)	CTAB (g)	pH	Ca/P (molar ratio)
1	90	1	11	1.30
2	90	0.3	11	1.30
3	90	0	11	1.30
4	25	1	11	1.30
5	60	1	11	1.30
6	90	1	6	1.30
7	90	1	7.4	1.30
8	90	1	11	1.50
9	90	1	11	1.67

2.2 Characterizations

The phase characterization of the powders was investigated by X-ray diffraction (XRD) analysis using D5000, Siemens with Cu Kα (λ=1.5418Å). The step size used in this study was 0.02, 2 seconds per step. Crystal size of the powder was calculated by the Rietveld method. Scanning electron microscopy (LEO 1550-SEM) was used to study the morphology of these bulk powders, and transmission electron microscopy (TEM) was performed using a Titan 80-300 (FEI Company, The Netherlands) operated in high angle annular dark field (HAADF) scanning TEM mode at 300 kV. The sample was analysed using X-ray photo electron spectroscopy (XPS, Quantum 2000, Al Kα X-ray source, Physical Electronics Inc., USA). C1s and Ca2p spectra were acquired from the area of size 100 × 100 m^2. Powders were deposited on a flat Ti surface. The sample has been sputtered before the first scan to remove contaminations on surfaces.

2.3 Small Angle X-ray scattering (SAXS)

The SAXS experiment was carried out on the I911-SAXS experimental beamline at MAX II storage ring of Max IV laboratory, Lund, Sweden.[34] A monochromatic X-ray beam (wavelength 0.91 Å) was used to illuminate the samples with the beam size of 0.3(h) x 0.3(v) mm^2. Downstream of the beam a Pilatus 1 M detector was positioned at a distance of 1905 ± 1 mm to collect the SAXS patterns. The data was analyzed by the free software DPDAK[35].

3. Results

As shown in Fig.1 a-d, synthesized monetite sheets had a nacreous-like structure, consisting of single monetite 'pages'. The width of monetite sheets was of 5-20 µm and the thickness was approximately 1 µm. The surfaces of these monetite sheets were quite smooth, see Fig.1 b, c. Plate-like and flower-like monetite co-existed with the multilayered monetite. Some of flower-like monetite covered the edges and surfaces of the layered structure, see Fig.1 c and d, which indicated the orderly nacreous-like monetite might be originated from these plate-like and flower-like monetite structures. The plate-like monetite was quite thin and randomly oriented, see Fig.1 e. The flower-like monetite was composed of many nanosheets with different orientations, see Fig.1 f. X-ray diffraction patterns confirmed the synthesized sheets were single-phase monetite, see Fig.1 g. The nanolayer thickness is estimated around 2.6 nm on a basis of the SAXS peak position by equation $d = \frac{2\pi}{q}$, shown in Fig. 1 h.

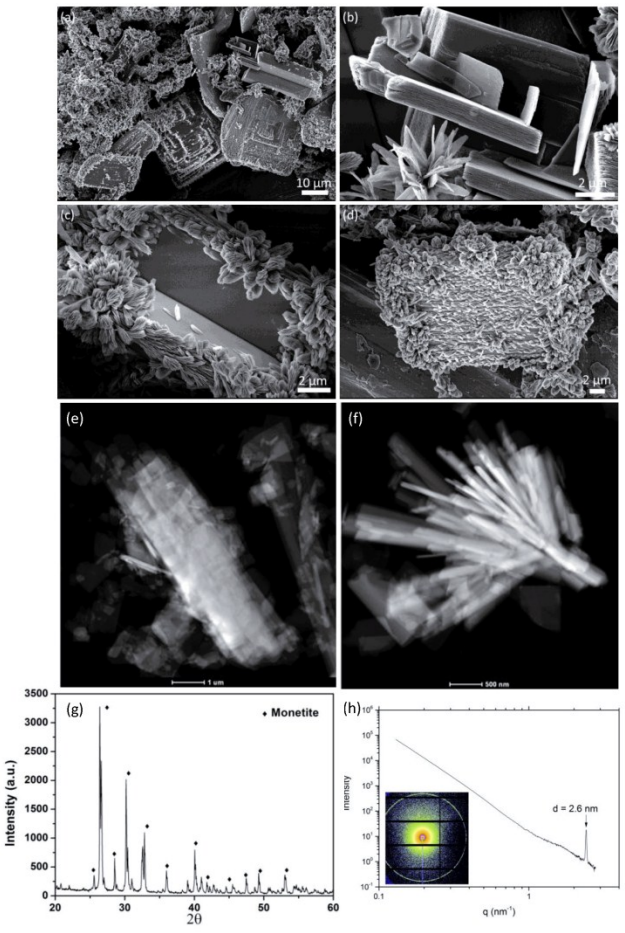

Fig. 1 Characterization of typical monetite sheets synthesized at 90 °C, pH=11 for 3h. (a-d) SEM micrographs. (e) STEM HAADF image showing overlapping nanosheets. (f) STEM HAADF image of flower-like monetite assembled from nanosheets. (g) X-ray diffraction pattern. (h) Synchrotron radiation result showing the distance between the layers was 2.6 nm.

To explore the mechanism of forming such nacreous-like monetite, we altered the temperature, pH and stirring time during synthesis to determine how these parameters affected the hierarchical structure of monetite. Variations of parameters were shown in Table 1. Despite of variations in these parameters, the resultant crystals were all single-phase monetite, see Fig.2 i. However, without CTAB, only irregular sheet-like monetite could be observed, see Fig.2 a. Nacreous-like monetite could be observed at lower concentration of CTAB (1.2%), indicating that CTAB was essential in forming such hierarchical structures, see Fig.2 b.

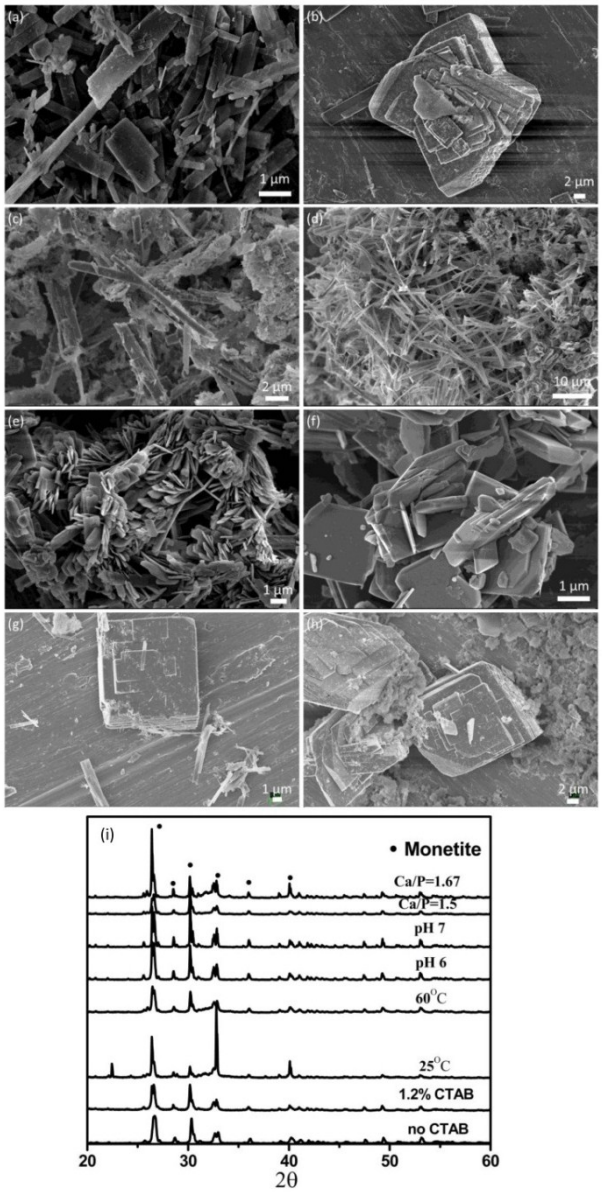

Fig. 2 SEM images of monetite synthesized for 3 h. (a) pH 11, 90°C, Ca/P=1.3,without CTAB (b) pH 11, 90°C, Ca/P=1.3,0.3 g CTAB (c) pH 11, 25°C, Ca/P=1.3,1 g CTAB (d) pH 11, 60°C, Ca/P=1.3, 1 g CTAB (e) pH=6, 90 °C, Ca/P=1.3, 1 g CTAB (f) pH=7, 90 °C, Ca/P=1.3, 1 g CTAB (g) pH 11, 90°C, Ca/P=1.5, 1 g CTAB (h) pH 11, 90°C ,Ca/P=1.67, 1 g CTAB (i) Corresponding X-ray diffraction pattern of monetite in (a)-(h).

As shown in Fig.2 c and d, temperature also plays a vital role in the self-assembly process of monetite. Plate-like and irregular monetite can be observed at 25 °C, see Fig.2 c. At higher temperature (60°C), the morphology of monetite became whisker-like, see Fig.2 d.

Monetite is one of the most thermodynamically stable phases among calcium orthophosphate compounds under pH 4. When forming nacreous-like monetite, the final pH of the solution after reaction was 4.2. The morphology of monetite changed with initial pH of the $Ca(NO_3)_2$ solution. The resultant crystals were stacked-sheet under pH 6 (Fig.2 e) and plate-like under pH 7 (Fig.2 f), indicating that lower pH of precursor solution might interrupt the interaction between the inorganic-organic components during the process of nucleation. Thus, no self-assembly process can be observed after the reaction. Adjusting the Ca/P molar ratio to 1.5 and 1.67, ordered layered and plate-like monetite coexisted which is similar to that of Ca/P=1.3 see Fig.2 g, h.

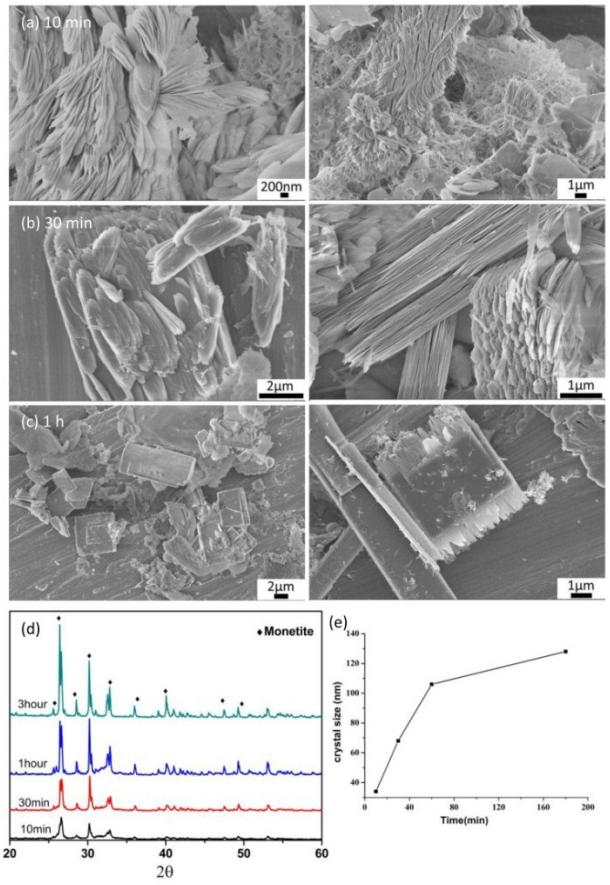

Fig. 3 SEM micrographs of monetite synthesized at 90°C, pH=11, Ca/P=1.3, 1 g CTAB stiring for (a) 10min, (b) 0.5h, (c)1h, (d) X-ray diffraction pattern of monetite powders of (a) , (b) and (c). (e) Crystal size calculated from X-ray diffraction (XRD) data.

To obtain a deeper understanding of the self-assembly process of nacreous-like monetite, powders at different time points were taken out and analyzed using XRD and SEM, see

Fig.3. For all time points, resultant crystals were single-phase monetite, see Fig.3 d.

However, the morphology of the monetite changed with the stirring time. Regular plate-like monetite occurred and started to assemble after 10min stirring, see Fig.3 a. After 30 min stirring, well-stacked monetite can be observed, see Fig.3 b. After stirring for 1h, these stacked monetite continue to grow and intact monetite with a nacreous-like structure was formed, see Fig.3 c. The crystal size was around 35 nm after 10 min stirring and it continued to grow during the 3 hours, see Fig.3 e. The average crystal size was 128 nm after 3 hours stirring.

The concentration of precursor solution (3M $Ca(NO_3)_2{\cdot}4H_2O$) was relatively high in the experiment, above which it might prevent the diffusion of Ca^{2+} and $H_2PO_4^-$ in the solution. Therefore, different morphologies coexisted in the powders prepared above. In order to obtain a homogeneous layered structure, the concentration of the solution was 30 times decreased. Under lower concentration the monetite sheets were stacked with well-oriented small fibers, see Fig.4. These sheets were 10μm long, 5 μm wide and 3 μm in thickness.

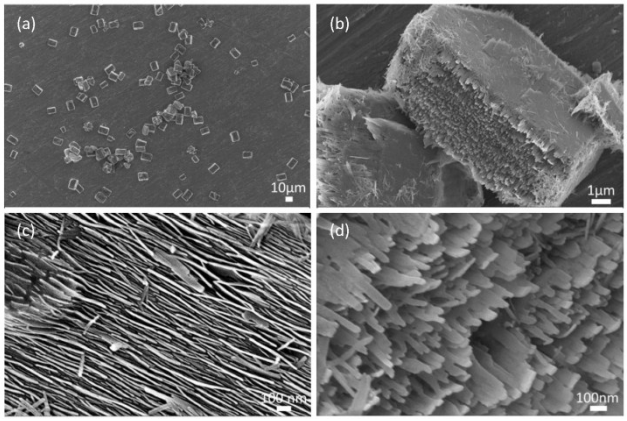

Fig. 4 SEM micrographs of monetite sheets synthesized at lower concentration of precursor solution (0.1M $Ca(NO_3)_2{\cdot}4H_2O$) , stirring for 3h, pH 11, 90℃, Ca/P=1.3,1 g CTAB.

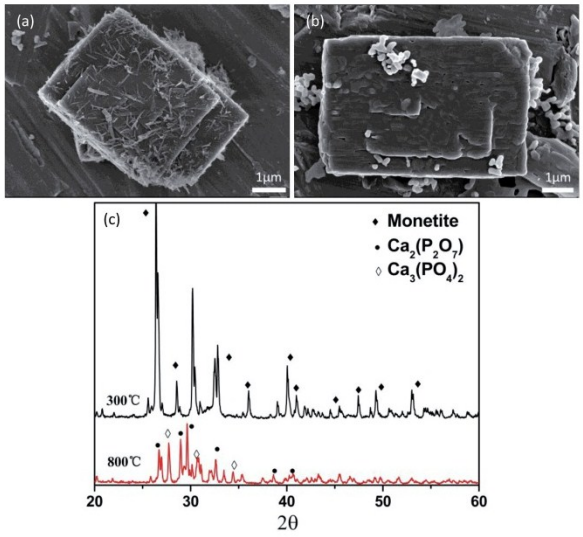

Fig. 5 SEM micrographs of monetite sheets synthesized at 90°C, pH=11 for 3h, post heating at (a) 300 °C, (b) 800 °C, (c) X-ray diffraction patterns of (a) and (b).

Table 2 shows the unit cell dimensions of the two final mateials (Fig. 1b and Fig. 4b). Compared to the data from ICDD (04-009-3755), all parameters are almost the same. The thermal stability of monetite sheets was studied by heating the sheets up to 300 °C and 800 °C. The X-ray diffraction patterns showed that monetite sheets were still single-phase monetite after heating at 300 °C. Increasing the temperature to 800°C, the main phase shifted to $Ca_2P_2O_7$, see Fig.5 c. Usually, monetite is stable below 400 °C and starts to transfer to $Ca_2P_2O_7$ at 430 °C.[20] The SEM image showed the boundary of the sheets started to melt at 800 °C, see Fig.5 b.

The Ca2p and C1s peaks after pre-sputtering and the second sputtering are shown in Fig.6. The binding energy of the Ca2p3/2 peaks is 347.6 eV, which is in agreement with values for tri-calcium phosphate. The C1s peak appears at a binding energy of 385.2eV for pre-sputtering, and 384.8 eV for the second sputtering, which indicates C-C or C-H bonding from CTAB.

Table 2 Unit cell dimensions of monetite nanosheets

Parameters	*a* (Å)	*b* (Å)	*c* (Å)	α (°)	β (°)	γ (°)
Monetite with sheets	6.90	6.64	6.99	96.2	104.0	88.5
Monetite with fibers	6.90	6.63	6.99	96.2	104.0	88.4

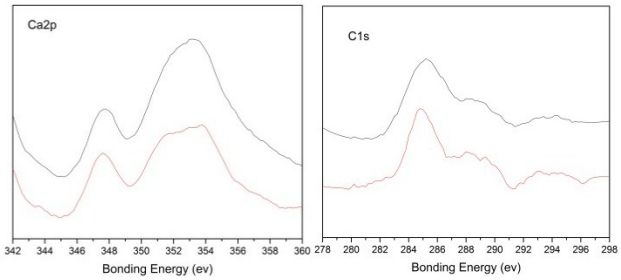

Fig. 6 The XPS spectra of Ca2p (A) and C1s (B) of monetite nanosheets. Black: First scan after pre-sputtering. Red: Second scan after a second sputtering.

4. Discussion

The chemical reaction to form $CaHPO_4$ can be described as follow: $Ca^{2+} + H_2PO_4^- = CaHPO_4 + H^+$. $CaHPO_4$ is triclinic pinacoidal with the unit-cell dimension: a=6.90Å, b=6.65Å, c=7.00Å, α=96°21′, β=103°54′, γ=88°44′. In monetite, PO_4^{3-} tetrahedral forms the three-dimensional network with Ca^{2+} in the interstice which bonds with oxygen atoms by strong ionic bonds.[36] As reported by other researchers, plate-like monetite is the most common morphology prepared by aqueous solution methods.[37] In our work, fiber and plate-like monetite can be observed during the synthesis and these fibers and plates can further form well-ordered structure under proper pH, temperature and stirring time. Then it comes to the question how the monetite assembles to form nacreous-like structures. George Whitesides divided self-assembly systems into two kinds: static and dynamic.[33] In both of the systems, energies are required to form the ordered structure. The energy can be provided by ultrasonic-radiation through which oriented assemblies of monetite nanosheets were synthesized.[38] In this experiment, 90 °C was required to initialize the self-assembly process and no self-assembly process can be observed when the temperature was lower than 60 °C. This indicates that reaction temperature is one of the key parameter for the self-assembly process. The results

show the presence of CTAB was not the key of influencing the morphology of monetite. However, CTAB did affect the assembly process of nacreous-like structures. The XPS analysis proved the presence of carbon in the nanosheets. As stated by other researchers[3], organic molecules play two different roles in the process of forming a nacreous layer: one is to control polymorphism and crystal size, while the other is to inhibit the crystal growth and promote the formation of mineral bridge between sheets. Here, CTAB plays both roles respectively: some CTAB molecules can strongly interact with monetite crystals due to the bond between $H_2PO_4^-$ and CTAB head group, which greatly reduces the interfacial free energy of the system. These tightly bond CTAB regulated the morphology of moneite crystals to plate-like or fiber-like building blocks, see Fig.7 a. The extra CTAB molecules in the solution limit the motion of Ca^{2+} and $H_2PO_4^-$ ions thus inhibit the further growth of these monetite crystals. At the same time, mineral bridges form between the building blocks to form single layer $CaHPO_4$, see Fig.7 b. Under constant stirring and heating, the oriented single layers assemble to form nacreous-layer structures, see Fig.7 c.

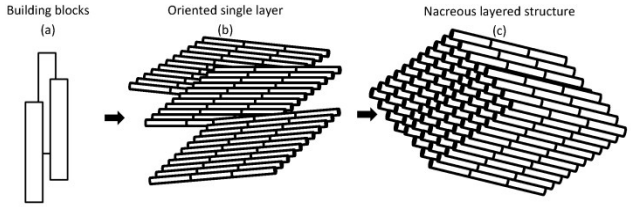

Fig. 7 Schematic illustration on the formation of nacreous layered monetite sheets. Under high concentration of precursor solution (3M $Ca(NO_3)_2{\cdot}4H_2O$), the building blocks were nano plates. Under lower concentration of precursor solution (0.1M $Ca(NO_3)2{\cdot}4H_2O$), the building blocks were nano fibers.

5. Conclusions

In summary, thin nacreous-like monetite sheets were successfully synthesized in the presence of CTAB. The nacreous-like monetite sheets can be stacked either from nano sheets or fibers. The distance between nano layers is around 2.6 nm. Temperature, initial pH and the concentration of CTAB are important in forming these hierarchical structures. In order to achieve monetite with a nacreous structure, the temperature should be higher than 90 °C and the reaction should be carried out in a basic solution guided by CTAB.

ACKNOWLEDGEMENTS

We appreciate the support from VR (Swedish Research Council (2013-5419)) and the China Scholarship Council (CSC) for supporting S.C. in his PhD studies. TEM was carried out at the Canadian Centre for Electron Microscopy at McMaster University. S.Y acknowledges the kind financial support from Knut och Alice Wallenberg foundation. MAX-IV Laboratory is acknowledged for beamtime and beamline staffs at beamline I911-SAXS at MAX-II storage ring are acknowledged for the support.

REFERENCE

1. I. Corni, T. J. Harvey, J. A. Wharton, K. R. Stokes, F. C. Walsh and R. J. Wood, *Bioinspiration & biomimetics*, 2012, **7**, 031001.
2. Z. R. Tian, J. A. Voigt, J. Liu, B. McKenzie, M. J. McDermott, M. A. Rodriguez, H. Konishi and H. Xu, *Nature materials*, 2003, **2**, 821-826.
3. Y. Oaki and H. Imai, *Angewandte Chemie*, 2005, **44**, 6571-6575.
4. Y. H. Tseng, H. Y. Lin, M. H. Liu, Y. F. Chen and C. Y. Mou, *J Phys Chem C*, 2009, **113**, 18053-18061.
5. N. Gehrke, N. Nassif, N. Pinna, M. Antonietti, H. S. Gupta and H. Colfen, *Chem Mater*, 2005, **17**, 6514-6516.
6. Y.N. Xia, P.D. Yang, Y.G. Sun, Y.Y. Wu, B. Mayers, B. Gates, Y.D. Yin, F. Kim and H. Yan, Advanced Materials, 2003, 15, 353-389.
7. M. A. Meyers, J. McKittrick and P. Y. Chen, *Science*, 2013, **339**, 773-779.
8. C. Yao, A. Xie, Y. Shen, J. Zhu and H. Li, *Materials science & engineering. C, Materials for biological applications*, 2015, **51**, 274-278.
9. X. Q. Li and H. C. Zeng, *Adv Mater*, 2012, **24**, 6277-6282.
10. R. Z. LeGeros, *Chemical reviews*, 2008, **108**, 4742-4753.
11. T. Kokubo, Bioceramics and their clinicla applications, CRC press, New York, 2008.
12. L. Medvecky, M. Giretova and T. Sopcak, *Materials Letters*, 2013, **100**, 137-140.
13. A. C. Tas, *Journal of the American Ceramic Society*, 2009, **92**, 2907-2912.
14. F. Tamimi, Z. Sheikh and J. Barralet, *Acta biomaterialia*, 2012, **8**, 474-487.
15. F. Tamimi, J. Torres, D. Bassett, J. Barralet and E. L. Cabarcos, *Biomaterials*, 2010, **31**, 2762-2769.
16. F. Tamimi, J. Torres, C. Kathan, R. Baca, C. Clemente, L. Blanco and E. Lopez Cabarcos, *Journal of biomedical materials research. Part A*, 2008, **87**, 980-985.
17. O. Suzuki, M. Nakamura, Y. Miyasaka, M. Kagayama and M. Sakurai, *The Tohoku journal of experimental medicine*, 1991, **164**, 37-50.
18. M. C. Ball and M. J. Casson, *Journal of the Chemical Society* 1973, **1**, 34-37.
19. H.McDowell, W.E.Brown and J.R.Sutter, *Inorganic Chemistry*, 1970, **10**, 1638-1643.
20. J. G. Rabatin, R. H. Gale and A. E. Newkirk, *The Journal of Physical Chemistry*, 1960, **64**, 491-493.
21. Z. Zou, X. Liu, L. Chen, K. Lin and J. Chang, *Journal of Materials Chemistry*, 2012, **22**, 22637.
22. S. Jinawath, D. Pongkao, W. Suchanek and M. Yoshimura, *International Journal of Inorganic Materials*, 2001, **3**, 997-1001.
23. B. Jokić, M. Mitrić, V. Radmilović, S. Drmanić, R. Petrović and D. Janaćković, *Ceramics International*, 2011, **37**, 167-173.
24. Y. Tokuoka, Y. Ito, K. Kitahara, Y. Niikura, A. Ochiai and N. Kawashima, *Chemistry Letters*, 2006, **35**, 1220-1221.
25. H. Eshtiagh-Hosseini, M. R. Houssaindokht, M. Chahkandhi and A. Youssefi, *Journal of Non-Crystalline Solids*, 2008, **354**, 3854-3857.
26. G. Thomas and H. Dehbi, *Materials Chemistry and Physics*, 1986, **15**, 1-13.
27. H. H. K. Xu, L. Sun, M. D. Weir, J. M. Antonucci, S. Takagi, L. C. Chow and M. Peltz, *Journal of Dental Research*, 2006, **85**, 722-727.

28. G. G. Chen, G. S. Luo, L. M. Yang, J. H. Xu, Y. Sun and J. D. Wang, *Journal of Crystal Growth*, 2005, **279**, 501-507.
29. X.-D. Kong, X.-D. Sun, J.-B. Lu and F.-Z. Cui, *Current Applied Physics*, 2005, **5**, 519-521.
30. K. Wei, C. Lai and Y. Wang, *Journal of Materials Science*, 2007, **42**, 5340-5346.
31. M.-G. Ma, Y.-J. Zhu and a. J. Chang, *Journal of Physical Chemistry B*, 2006, **110**, 14226-14230.
32. S. Sanchez-Salcedo, J. Werner and M. Vallet-Regi, *Acta biomaterialia*, 2008, **4**, 913-922.
33. G. M. Whitesides and B. Grzybowski, *Science*, 2002, **295**, 2418-2421.
34. A. Labrador, Y. Cerenius, C. Svensson, K. Theodor and T. Plivelic, *Journal of Physics: Conference Series*, 2013, **425**, 072019.
35. G. Benecke, W. Wagermaier, C. Li, M. Schwartzkopf, G. Flucke, R. Hoerth, I. Zizak, M. Burghammer, E. Metwalli, P. Muller-Buschbaum, M. Trebbin, S. Forster, O. Paris, S. V. Roth and P. Fratzl, *Journal of applied crystallography*, 2014, **47**, 1797-1803.
36. C. A. B. G. MAcLennan, *Acta Crystallographica*, 1955, **8**, 579-583.
37. H. Ito, Y. Oaki and H. Imai, *Crystal Growth & Design*, 2008, **8**, 1055-1059.
38. Q. Ruan, Y. Zhu, Y. Zeng, H. Qian, J. Xiao, F. Xu, L. Zhang and D. Zhao, *J.Phys.Chem.B*, 2009, **113**, 1100-1106.